Segmental Analysis of the Transmission in CSK Systems Based on the Euclidean Distance

A. R. Ndjiongue†, H. C. Ferreira† and A. J. Han Vinck*
†Department of Electrical and Electronic Engineering Science, University of Johannesburg,
*Institute of Experimental Mathematics, University of Duisburg-Essen,
Emails: {arrichard,hcferreira}@uj.ac.za,vinck@iem.uni-due.de

***Abstract*—This article presents a segmental analysis of the transmission in colour shift keying (CSK). The Euclidean distance is fractionally studied to find the distance limits between the observed and the expected points. Practical segmental characterisation of the CSK receiver is presented to verify the Voronoi segmentation over the CSK channel and confirm crosstalk and correlation between the red, green and blue channels based on the threshold selection.**

***Index Terms*—CSK, Euclidean distance, constellation, RGB-LED, chromaticity, optimal detection.**

I. Introduction and background

In visible light communications (VLC), a light bulb is used to couple the telecommunication signal into the channel. VLC uses the visible spectrum to transmit data by modulating the intensity of the light. Many modulation techniques are available to be used in VLC, such as on-off keying (OOK), variable pulse position modulation (VPPM), colour shift keying (CSK), to mention only a few [1]. CSK is a modulation scheme in which symbols are converted into colours. This scheme presents some advantages when compared to other modulation techniques [2]. The design of a CSK system is subject to many constraints such as the illumination constancy and dimming requirements [3], [4]. Constellation design for colour shift keying are proposed in the literature [3] - [5].

Many methods are available to be used to evaluate the distance between two points. Among them, we distinguish the Euclidean distance, the Manhattan distance, the correlation method, the dynamic time wrapping (DTW), the longest common subsequence (LCSS). Euclidean theorem of distance is the most used method to estimate the distance between points. It is suitable for metric distance functions. It respects properties such as positivity, symmetry and triangle inequality [6], [7].

In most research in CSK constellation design, the minimum distance is estimated on the xy chromaticity coordinates of the colours [1] (The xy chromaticity plane was created by the international commission on illumination (CIE) in 1931). Nevertheless, in [8], an analysis of the performance of IEEE 802.15.7 CSK modulation is proposed based on the Voronoi segmentation of the constellation triangle. In this article, we propose a segmental analysis of the Euclidean distance in CSK based on the threshold selection. This will allow us to investigate the probabilities in matching the sent and the received constellations. We practically look at the correlation between the three channels provided by the CSK method. We also look at the influence of the three channel noise on the symbol error rate (SER).

We revisit the CSK constellation design and the CSK channel in Section II. In Section III, we propose a segmental analysis of the CSK transmission. The next section presents the practical characterisation of a CSK receiver. We analyse the transmission over the CSK channel in the $(\vec{r},\vec{g},\vec{b})$ plane and propose the SER performance per channel. Concluding remarks are given in Section V.

II. Overview of the CSK transmission and design considerations

A. The CSK channel

In communication, when the system is corrupted by additive white Gaussian noise (AWGN), the transmission is governed by

$$r_j = \mathbf{H}s_j + n, \tag{1}$$

where r_j and s_j are the j^{th} received and the j^{th} transmitted symbols, respectively. $\mathbf{H}$ is the matrix representing the channel transfer function and n is the noise vector. The size of the matrix $\mathbf{H}$ depends on the number of streams used for the transmission. $\mathbf{H}$ also varies with the line-of-sight (LOS) situation over the communication environment [9]. In VLC, the single channel is determined by the use of a single colour-LED and a single photodetector (PD) to achieve transmission, while, the multi-channel uses more than one colour-LED [9]. A general view of the channel matrix in CSK is analysed and given in [5]. In general, considering the actual availability of multi-colour-LEDs, red-green-blue light emitting diodes (RGB-LEDs) are mostly used in CSK design. In this case, $\mathbf{H}$ is a 3×3 matrix given by

$$\mathbf{H} = \begin{pmatrix} \gamma_{rr} & \gamma_{rg} & \gamma_{rb} \\ \gamma_{gr} & \gamma_{gg} & \gamma_{gb} \\ \gamma_{br} & \gamma_{bg} & \gamma_{bb} \end{pmatrix}, \tag{2}$$

where the diagonal entries γ_{rr}, γ_{gg} and γ_{bb} represent the front-end gain between each colour-LED and the corresponding PD, and, the rest of entries represents the crosstalk gain between channels [5], [9] and [10]. Many sources of noise are identified. Among them, shot and thermal noise are the most important. Each of the three channels of the CSK system is affected by a different component of the noise. Fig. 1 depicts a CSK transmission system using a single RGB-LED and a

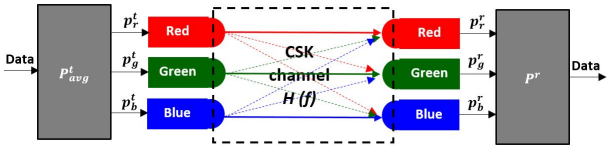

Figure 1. The colour shift keying (CSK) transmission system: a single RGB-LED is used to transmit data and a single pixel colour sensor is used as receiving antenna.

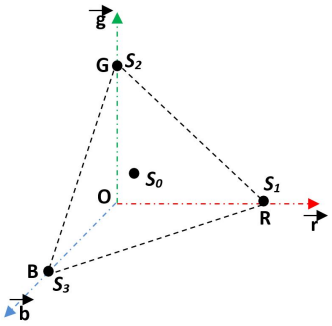

Figure 2. Convex polytope representing the $(\vec{r}, \vec{g}, \vec{b})$ orthogonal plane highlighting the CSK constraint region.

single pixel colour sensor [10]. It highlights the presence of crosstalk in a CSK communication system.

B. CSK design considerations

Let **s**, **c** and **r** be the incoming data set, the set of colours and the received alphabet, respectively. **s** is mapped to **c** and each colour is produced by applying three different current intensities to the RGB-LED. The transmission should be achieved taking into account the constraints of the CSK constellation design, which are the constant illumination, the chromaticity constraint and the communication throughput. The average transmit optical power P^t_{avg} must remain constant within the transmitted alphabet, the minimum distance between two symbols must be maximised [1], [9] and [10], and the average colour must be kept constant while maximising the communication efficiency. To achieve transmission under these conditions, the final produced colour must fit in the triangle delimited by the three basic colours red, green and blue shown in Fig. 2 [1].

III. Segmental analysis and probabilistic decision

At least three systems can be used to analyse transmission in CSK: the CIE xy chromaticity plane, the CIE XYZ colour system, and the RGB colour space. For a colour $c_i \in \mathbf{c}$, X_i, Y_i and Z_i are the tristimulus values of c_i. They can be calculated using the power distribution of c_i related to the colour wavelength and its frequency. The xy coordinates of a colour are derived from the XYZ system and represent the colour in the chromaticity plane. Each xy coordinate can be represented using XYZ by $x = X/(X+Y+Z)$ and $y = Y/(X+Y+Z)$. In general, the RGB colour space is used to generate the current intensities needed to produce the colour. The RGB and XYZ colour spaces are linked. Hence, the transmission in CSK can be analysed in the RGB colour space, providing the opportunity to analyse the three different channels.

A. segmental analysis and optimisation

The convex polytope shown in Fig. 2 has three main vertices normalised by the norms of the three vectors $\vec{r}$, $\vec{g}$ and $\vec{b}$. We look at the distance between the j^{th} observed symbol r_j and the j^{th} expected symbol e_j $(j = 0, 1, 2, \ldots, M-1)$. This will give the probability of receiving e_j instead of $\mathbf{H}s_j$. This probability can be optimised by maximising the minimum distance between two symbols on the sender constellation as presented in [5]. During transmission, the point s_j is shifted to a new position r_j. We evaluate the distance $d_{s_j r_j}$ between s_j and r_j. By definition, $d_{s_j r_j}$ is given by

$$d_{s_j r_j} = \|s_{rj} - r_{rj}\|^2 + \|s_{gj} - r_{gj}\|^2 + \|s_{bj} - r_{bj}\|^2, \quad (3)$$

where s_{rj}, s_{gj} and s_{bj} are the intensities of the transmitted colour s_j, and, r_{rj}, r_{gj} and r_{bj} are the intensities of the received colour r_j, respectively. A correct decision is achieved when the noise does not move the received vector outside the Voronoi region. The objective of the design is then to minimise the maximum likelihood Euclidean distance between the transmitted and the received sets **s** and **r**, respectively. This can be achieved by applying the maximum a posteriori probability (MAP) detection rule given by

$$\varpi = argMax\mathbf{P}\{\mathbf{s}\ sent|\mathbf{r}\ received\}. \quad (4)$$

When the transmission is dominated by AWGN, the apriori message probabilities are all equal, then, the optimum receiver has to minimise the squared Euclidean distance metric target on the point r_j [5], [11] and [12] by

$$\varpi = argMin\{\|e_j - \mathbf{H}s_j\|^2\}, \quad (5)$$

knowing that the minimum distance between r_j and s_j is upper-bounded by $Q[(\|e_j - \mathbf{H}s_j\|)/(2\sqrt{N_0/2})]$, where $\|e_j - \mathbf{H}s_j\|)$ represents the distance from the two vectors e_j and s_j to the decision boundary. This shows that the probability depends on the distance between the two signal points. The objective function $\|e_j - \mathbf{H}s_j\|^2$ is rearranged using a decision variable ϕ [4], [5]. The optimum detection of the received set of points is then given by

$$\varpi = argMin\{\|\mathbf{e}(\phi) - \mathbf{Hs}(\phi)\|^2\}, \quad (6)$$

where $\mathbf{e}(\phi)$ is the expectation set. The function of the decision variable ϕ must meet the requirements and the constraints of the CSK constellation design. To achieve the communication objectives, we write the distance $d_{s_j r_j}$, which is proportional to the detection probability as

$$\begin{aligned} d_{s_j r_j} &= \|r_j - s_j\|(received - sent) \\ &= \|e_j - \mathbf{H}s_j\|(expected - detected). \end{aligned} \quad (7)$$

We square $d_{s_j r_j}$, compare it to (3), and obtain

$$\|e_j - \mathbf{H}s_j\|^2 = \|e_{rj} - \mathbf{H}s_{rj}\|^2 + \|e_{gj} - \mathbf{H}s_{gj}\|^2 + \|e_{bj} - \mathbf{H}s_{bj}\|^2, \quad (8)$$

where $\mathbf{H}_r$, $\mathbf{H}_g$ and $\mathbf{H}_b$ represent the channel impulse responses of the bands red, green and blue, respectively. e_{rj}, e_{gj} and e_{bj} are the red, green and blue intensities of the j^{th} expected colour. Hence, the minimum of the squared Euclidean distance metric between s_j and r_j can be split into three parts as

$$Min\|e_j - \mathbf{H}s_j\|^2 = \sum_{\alpha}\{Min\|e_{\alpha j} - \mathbf{H}s_{\alpha j}\|^2\}, \quad (9)$$

where $\alpha = \{r, g, b\}$. Equation (9) being non-differentiable, it is then important to find its approximation [5], [10]. Based on (6), we use a differentiable equation that approximate (5) and satisfy (4). The following objective function fits better to the above description of the described objective detection situation [5], [10].

$$\frac{ln}{\beta}\sum exp(-\beta\|e_j - \mathbf{H}s_j\|^2). \quad (10)$$

The function (10), according to [5] is a function of the decision variable ϕ, since its solution satisfies the maximum detection probability. Hence, we can write and redistribute $f(\phi)$ over the RGB colour space as

$$f(\phi) = \frac{ln}{\beta}\sum\sum_{\alpha} exp(-\beta\|e_{\alpha j}(\phi) - \mathbf{H}_\alpha s_{\alpha j}(\phi)\|^2). \quad (11)$$

B. 3D expectation and density function

It is evident that (8), (9) and (11) represent a sum of three different channels. This gives us the opportunity to see the channel matrix as a matrix grouping the three matrices $\mathbf{H}_r$, $\mathbf{H}_g$ and $\mathbf{H}_b$. Since these matrices are not equal, we define three different decision regions with three different probabilities. The total probability has three components. This explains the reason of distributing the squared Euclidean distance in (8) in three small parts. Consequently, the correct decision defines a value ψ such that the j^{th} observed symbol $\mathbf{H}s_j$ lies in the very small interval between e_j and $e_j + \psi$. The definition of the probability density function can then be given from the three-dimensional $(\vec{r}, \vec{g}, \vec{b})$ system, and the corresponding Voronoi region is a three dimensional space having three components. Fig. 3 represents an example illustrating the decision region in 4CSK. The transmission cube is divided into four small pieces $\mathbf{v}_1$, $\mathbf{v}_2$, $\mathbf{v}_3$ and $\mathbf{v}_4$, each of them representing the boundaries of the received symbol when a correct decision is made. Thus, each symbol should belong to a distinct decision region. Each of $\mathbf{v}_1$, $\mathbf{v}_2$, $\mathbf{v}_3$ and $\mathbf{v}_4$ consists of a piece of sector formed by the transmitted and the expected sets. We can then fractionally redistribute the expected interval $[e_j, e_j + \psi]$ into the three axis of the $(\vec{r}, \vec{g}, \vec{b})$ space as shown in Fig. 3. In this figure, the symbol s_j, represented by its coordinates s_{rj}, s_{gj} and s_{bj} will be correctly transmitted if the corresponding observed symbol $\mathbf{H}s_j$, stays in the three dimensional space delimited by the three intervals $[\psi_{rj}]$, $[\psi_{gj}]$ and $[\psi_{bj}]$. The volume of the cube is influenced by the channels impairment sources. The volume-to-noise ratio [13] can be computed to characterise the decision region. The probability function, for the j^{th} observed symbol

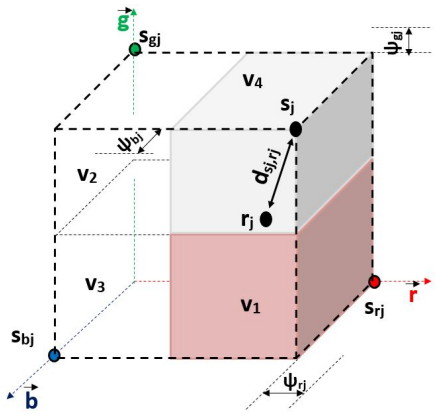

Figure 3. Decision region made of Voronoi cube limited by space interval characterising a correct decision, to transmit and receive symbols in a 4CSK

to be equal to the j^{th} expected symbol e_j is investigated and represented in the three dimensional $(\vec{r}, \vec{g}, \vec{b})$ space by

$$\mathbf{P}(\mathbf{H}s_j|e_j) = \frac{1}{(\pi N_0)^{3/2}} exp\left(-\sum_{\alpha=r,g,b}\frac{\|e_{\alpha j} - \mathbf{H}s_{\alpha j}\|^2}{N_0}\right). \quad (12)$$

C. Average energy

The average energy $\varepsilon_{avg,j}$ allocated to the j^{th} symbol s_j is an important characteristic of the transmission. $\varepsilon_{avg,j}$ is given by [9]

$$\varepsilon_{avg,j} = \frac{1}{M}\sum_{j=0}^{M-1}\|s_j\|^2. \quad (13)$$

$\varepsilon_{avg,j}$ can be seen as a 3-tuple signal related to s_{rj}, s_{gj} and s_{bj} due to the relationship $\|s_j\|^2 = \|s_{rj}\|^2 + \|s_{gj}\|^2 + \|s_{bj}\|^2$, therefore, we can write

$$\varepsilon_{avg,j} = \frac{1}{M}\sum_{j=0}^{M-1}\sum_{\alpha}\|s_{\alpha j}\|^2, \quad (14)$$

to quantify the amount of energy to be allocated to each of the three streams in a given symbol.

IV. Practical analysis

A. Implementation

Three RGB-LEDs of 3W each are used to light a single RGB colour sensor. The RGB-LEDs are characterised by the following rated values: red 2.5 V - 3 V, 350 mA, 20.7 lm, 620 - 630 nm, green and blue 3.2 V - 3.5 V, 350 mA, 16.5 lm, 520 - 530 and 460 - 470 nm, light diffusion beam 140^o. The PD is made of a single pixel RGB complementary metal-oxide semiconductor (CMOS) sensor. It is a high performance, small in size and cost effective light to voltage converting sensor. The sensor combines a photodiode array and three trans-impedance amplifiers in a single monolithic integrated circuit. Three colour filters are coated over the photodiode array. The irradiance responsibilities are 645 nm, 542 nm and 460 nm for the red, green and blue photodiodes, respectively.

We buffer a message in a microcontroller and deliver it to the RGB-LED at the frequency of 500 kHz, corresponding to 2 μs bit-period. We realise a 4CSK, which means four colour changes can be made during the transmission of one set of symbols. As shown in Fig. 2, the symbols are organised as: $s_1 \Longrightarrow$ red, $s_2 \Longrightarrow$ green, $s_2 \Longrightarrow$ blue and $s_0 \Longrightarrow$ the centroid of the RGB triangle. For the RGB-LEDs, we build the circuit depicted in Fig. 4. We have a series of three red, of three green and three blue LEDs, forming the three streams described earlier in this paper. We then inject in the three

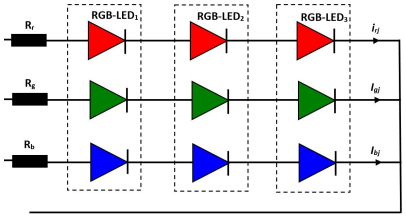

Figure 4. Combination of the RGB-LEDs in the built CSK transmitter

streams three different currents $[i_{rj}, i_{gj}, i_{bj}]$ depending on the final desired colour with j = 0,1,2,3. We impose [350, 0, 0] mA for transmitting s_1 under 2.75 V across each red LED to obtain about 2.887 W stream power. To transmit s_2 and s_3, we inject [0, 350, 0] mA and [0, 0, 350] mA into the circuit. This gives about 3.15 W per group of LEDs in series under 3.5 V across the green and blue LEDs. To transmit s_0, we inject [120.9, 129.63, 129.63] mA, by then, producing a total of 3.062 W. An average electric power of 3.06225 W is produced by the three streams of LEDs. Under the direct scattering diffusion of 140^o beam and 0^o incidence, a transmission distance of 100 cm is imposed between the RGB-LEDs and the PD.

B. Measurement

We power each stream of colour-LEDs individually. By varying each stream forward current, we measure the three output of the PD. The results are shown in Figs. 5, 6 and 7. They all confirm the behaviour of the CSK channel shown in Fig. 1, highlighting the presence of crosstalk between channels. When a single colour is transmitted, the corresponding detector shows increased sensitivity. Nevertheless, the two others detect a little light. This is due to a number of reasons: the PDs are not perfect, the single light transmitted does not have a pure colour, and, the background light from the sun rays affecting the diffusion of the selected colour. Fig. 8 shows the results in the case where the final colour is made of the three composite colours. The three detectors in the PD are all sensitive. The colour detected is a mixture of the original colours and the background light. Nevertheless, each detector in the CMOS sensor is sensitive to a specific wavelength. The situations described in Figs. 5, 6, 7 and 8 lead us to the segmentation of the detection region basing on the threshold selection. This is analysed for the detected current intensities and presented in Fig. 9. The detector takes into account only one current when the red, green or blue colours is transmitted, which is proportional to the optical intensity of the detected colour. It is represented by I_r, I_g or I_b in Fig. 9. The currents due to

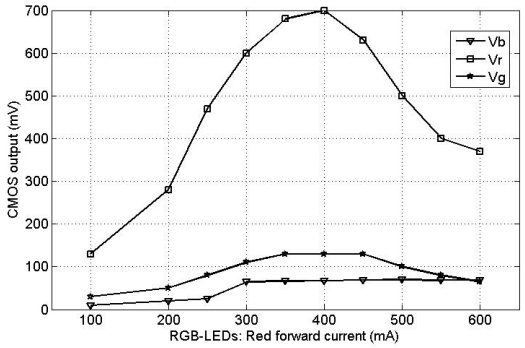

Figure 5. The CMOS colour sensor response under the influence of the light from the red LED

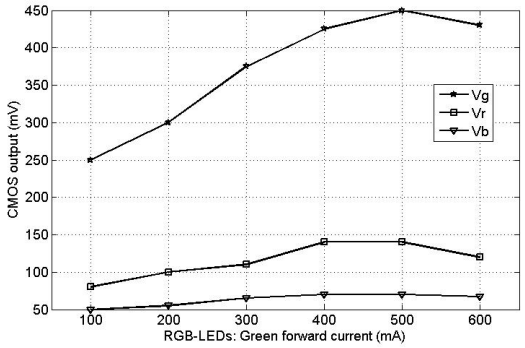

Figure 6. The CMOS colour sensor response under the influence of the light from the green LED

crosstalk represented by I_{0r}, I_{0g} or I_{0b} are to be neglected when they are lower than I_{min}. They are I_{mr}, I_{mg} and I_{mb} in Fig. 9. In the case that one of these crosstalk currents reaches the upper threshold I_{max}, the system will face errors in detecting s_1, s_2 or s_3. In the case of the transmission of s_0, the three currents detected should be bounded by I_{min} and I_{max}. If one of the three detected current is outside of the interval $[I_{min}, I_{max}]$, then the system faces errors in detecting s_0. Practically, we connect a 10 ohms resistor on the output of each colour sensor. A second microcontroller

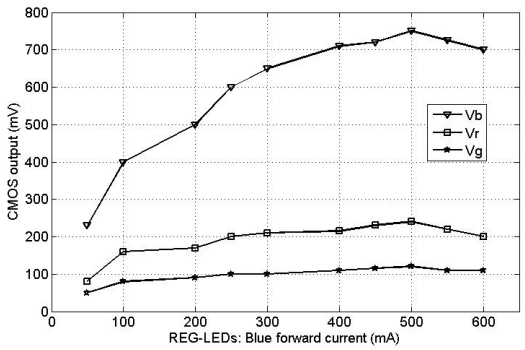

Figure 7. The CMOS colour sensor response under the influence of the light from the blue LED

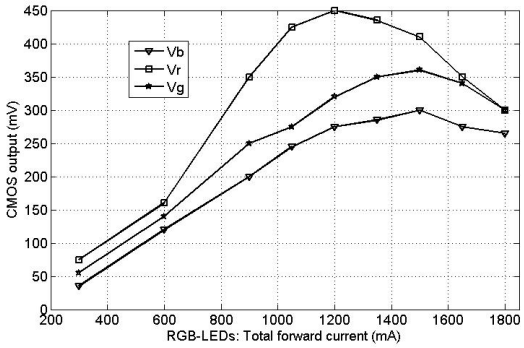

Figure 8. The CMOS colour sensor response under the influence of a mixture of light from the three LEDs

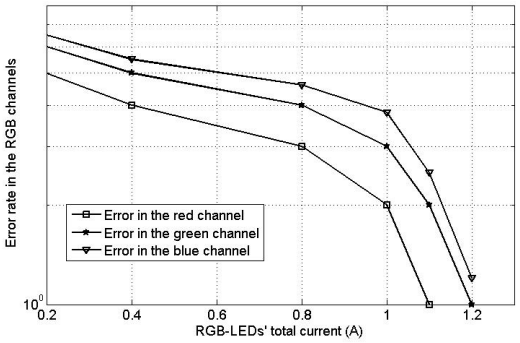

Figure 10. Segmented symbol error rate as a function of the LED current, under the background noise and an artificial flux interference of ...

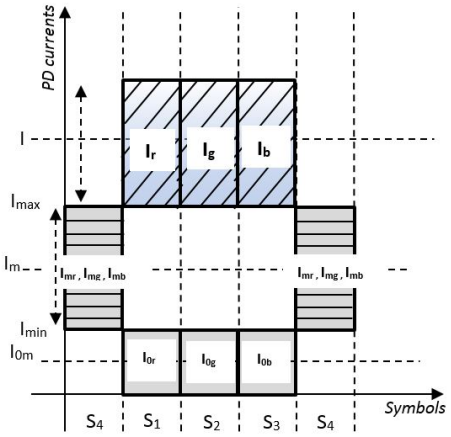

Figure 9. Current detection model for 4CSK highlighting the segmented decision threshold

measures the detected currents, compares their values with the lower and upper thresholds I_{min} = 20 mA and I_{max} = 40 mA respectively. We measured I_r = 70.111 mA, I_{0g} = 15.521 mA and I_{0b} = 5.067 mA to detect s_1. I_g = 63.551 mA, I_{0r} = 15.678 mA and I_{0b} = 8.457 mA for s_2, and I_b = 58,885 mA, I_{0r} = 25.235 mA and I_{0b} = 12.002 mA for s_3. The detection of s_0 is obtained with I_{mr} = 45.023 mA, I_{mg} = 34.766 mA and I_{mb} = 30.0125 mA. Now we inject into the channel a certain amount of light from an additional source. This additional source is built in the same way as the one in the transmitter. We power the additional source in such a way to obtain almost a white colour. When placed next to the transmitter, the second source considerably affects the channel. We record the behaviour of the receiver in Fig. 10, showing the correlation between the three channels. Thus, confirming that the correlation between the RGB channel presented for image processing [14] can be applied in CSK constellation design.

V. Conclusion

The transmission probability is analysed in a three dimensional system and the density function of the total probability is presented using three components. A single pixel colour sensor is characterised to establish the relation between the three channels and the symbol error rate for 4CSK is analysed. This work will help to evaluate the noise correlation between the channels in multiple scenarios that could occur over the CSK channel.

References

[1] "Ieee draft standard for information technology–telecommunications and information exchange between systems–local and metropolitan area networks–specific requirements–part 15.7: Phy and mac standard for short-range wireless optical communication using visible light," *IEEE P802.15.7/D4, November 2010*, pp. 1–296, Dec 2010.

[2] R. Roberts, S. Rajagopal, and S.-K. Lim, "Ieee 802.15.7 physical layer summary," in *GLOBECOM Workshops (GC Wkshps), 2011 IEEE*, Dec 2011, pp. 772–776.

[3] R. Drost and B. Sadler, "Constellation design for color-shift keying using billiards algorithms," in *GLOBECOM Workshops (GC Wkshps), 2010 IEEE*, Dec 2010, pp. 980–984.

[4] E. Monteiro and S. Hranilovic, "Constellation design for color-shift keying using interior point methods," in *Globecom Workshops (GC Wkshps), 2012 IEEE*, Dec 2012, pp. 1224–1228.

[5] R. Drost and B. Sadler, "Constellation design for channel precompensation in multi-wavelength visible light communications," *Communications, IEEE Transactions on*, vol. 62, no. 6, pp. 1995–2005, June 2014.

[6] A. S. Thakur and N. Sahayam, "Speech recognition using euclidean distance," *International Journal of Emerging Technology and Advanced Engineering*, vol. 3, no. 3, pp. 587–590, 2013.

[7] H. Breu, J. Gil, D. Kirkpatrick, and M. Werman, "Linear time euclidean distance transform algorithms," *Pattern Analysis and Machine Intelligence, IEEE Transactions on*, vol. 17, no. 5, pp. 529–533, May 1995.

[8] A. Halder and A. Barman, "Improved performance of colour shift keying using voronoi segmentation for indoor communication," in *Numerical Simulation of Optoelectronic Devices (NUSOD), 2014 14th International Conference on*, Sept 2014, pp. 109–110.

[9] A. ndjiongue, H. ferreira, and T. M. N. Ngatchedz, "Visible light communications (vlc) technology," in *Wiley Encyclopedia of Electrical and Electronics Engineering*, C. Strickland, Ed. John Wiley and Sons, 2015, accepted.

[10] E. Monteiro and S. Hranilovic, "Design and implementation of color-shift keying for visible light communications," *Lightwave Technology, Journal of*, vol. 32, no. 10, pp. 2053–2060, May 2014.

[11] F. Monteiro and I. Wassell, "Euclidean distances in quantized spaces with pre-stored components for mimo detection," in *Wireless Technologies, 2007 European Conference on*, Oct 2007, pp. 150–153.

[12] M. Zhang and Z. Zhang, "Fractionally spaced equalization in visible light communication," in *Wireless Communications and Networking Conference (WCNC), 2013 IEEE*, April 2013, pp. 4282–4287.

[13] A. Ingber, R. Zamir, and M. Feder, "The dispersion of infinite constellations," in *Information Theory Proceedings (ISIT), 2011 IEEE International Symposium on*, July 2011, pp. 1407–1411.

[14] A. Piva, F. Bartolinin, V. Cappellini, and M. Barni, "Exploiting the cross-correlation of rgb-channels for robust watermarking of color images," in *Image Processing, 1999. ICIP 99. Proceedings. 1999 International Conference on*, vol. 1, 1999, pp. 306–310 vol.1.